Article

Optical Evaluation of Intracorneal Ring Segment Surgery in Keratoconus

Nicolas Alejandre[1], Pablo Pérez-Merino[2], Gonzalo Velarde[1], Ignacio Jiménez-Alfaro[1], and Susana Marcos[3,4]

[1] Ophthalmology Department, Fundación Jiménez Díaz University Hospital, Madrid, Spain
[2] Centre for Microsystems Technology (CMST), Ghent University and Imec, Technologiepark, Ghent, Belgium
[3] Instituto de Óptica "Daza de Valdés", Consejo Superior de Investigaciones Científicas (CSIC), Madrid, Spain
[4] Center for Visual Science, The Institute of Optics, Flaum Eye Institute, University of Rochester, Rochester, New York, USA

Purpose: The purpose of this study was to assess the impact of different intracorneal ring segments (ICRS) combinations on corneal morphology and visual performance on patients with keratoconus.

Methods: A total of 124 eyes from 96 patients who underwent ICRS surgery were analyzed and classified into 7 groups based on ICRS disposition and the diameter of the surgical zone (5- and 6-mm). Pre- and postoperative complete ophthalmological examinations were conducted. Corneal geometry, volume, and symmetry were studied. Zernike polynomials were used to build a virtual ray-tracing model to evaluate optical aberrations and the Visual Strehl (VS).

Results: ICRS induced significant flattening across the cornea, being more pronounced on the anterior (+0.38 mm, $P < 0.001$) than on the posterior (+0.15 mm, $P < 0.001$) corneal radius. Asphericity experienced a larger change for a 6-mm surgical zone diameter (from -1.23 ± 1.1 to -1.86 ± 1.2, $P < 0.001$) than for a 5-mm zone (from -1.99 ± 1.1 to -2.10 ± 1.5, $P = 0.536$). Mean astigmatism was reduced by 2.05 D ($P < 0.001$). Combination four was the most effective in reducing astigmatism. Coma decreased by 30% on average and combination one produced an average reduction by 51% ($P < 0.05$). Patients experienced significant improvement in visual performance, best corrected visual acuity increased from 0.57 ± 0.21 to 0.69 ± 0.21 and VS changed from 0.049 ± 0.02 to 0.065 ± 0.041.

Conclusions: ICRS combinations implanted within 5 mm diameter zone are more effective in flattening the cornea, whereas those implanted on 6 mm diameter are as effective in reducing astigmatism and are a good choice if the asymmetry and the intended flattening are smaller. Combinations with asymmetrical implants are the best option to regularize corneal surface.

Translational Relevance: This study uses methods and metrics of optical research applied to daily clinical practice.

Introduction

Keratoconus is a progressive corneal disorder that affects the shape and structure of the cornea. The characteristic corneal thinning and irregular surfaces in patients with keratoconus severely impacts the final retinal image quality of the eye, making difficult its correction with spectacles or contact lenses.[1,2] To date, intracorneal ring segments (ICRS)[3–7] are increasingly used as a surgical option to improve the visual quality of patients with keratoconus and to delay corneal transplant. ICRS are polymethylmetacrylate (PMMA) segments with variable arc-length (90–340 degrees), width (150–350 µm), shape (triangular and hexagonal), and optical zone (5, 6, or 7 mm).

The segments are inserted in the corneal stroma through a manual or femtosecond laser made channel

according to a patient-oriented strategy and empirical nomograms. ICRS is a well-tolerated and effective treatment, offering in most cases long-term improvement in refractive and keratometric measurements.[7] However, surgical ICRS nomograms are generally qualitative and do not rely on a systematic mechanism of action of the corneal response to the potential different segment combinations implanted in the cornea. Recent studies have used corneal Finite Element Models to predict the changes in corneal curvature to virtually implanted ICRS,[8,9] and commercial software starts to become available to guide ICRS implantation (Optimo Medical AG: Optimeyes). Although predictive models are certainly the future, they still rely on limited experimental data on the mechanical properties of the keratoconic corneas.

Different studies have reported topographic changes in the anterior and posterior corneal surfaces after ICRS implantation from different corneal topography techniques: slit-scanning corneal topography,[10] Scheimpflug imaging[11] or optical coherence tomography.[12–14] Given the properties of keratoconic corneas (highly irregular with an asymmetric corneal thickness), dense lateral sampling and large range, micron axial resolution, and accurate anterior and posterior corneal elevation maps are required for pre- and postoperative evaluation of ICRS implantation. Most studies report flattening of the anterior cornea (with mean values of 2.5 D[15,16]), an unpredictable response of the posterior cornea (flattening[16]/steepening[17]), and, in general, a large intersubject variability in the postoperative corneal topography. Very few studies have evaluated systematically the ICRS-induced corneal changes in both anterior and posterior corneal surfaces, and in particular corneal aberrations and image quality metrics, in relation to the ICRS geometry and implantation parameters.[13] Accurate optical and geometric corneal characterization after ICRS implantation will not only increase knowledge on the contribution of each corneal surface to retinal image quality but will also give insights into the mechanism of action of the ICRS resulting in better estimation of postoperative corneal shape, and potentially, improvements in the predictability of the refractive outcomes and the implantation nomogram. Additional contributing factors to surgical outcomes include the corneal mechanical properties, the incision and tunnel technique, and the intrinsic variability in the manufacturing process of the implant.

In the current study, we measured pre- and postoperatively a large cohort of patients implanted with different ICRS combinations. Corneal elevation maps obtained with a commercially available corneal topography system (Pentacam, OCULUS Optikgeräte GmbH, Wetzlar, Germany) were incorporated in custom developed routines to estimate geometric parameters and in custom computer eye models that allowed estimation of ocular aberrations and retinal image quality.

Methods and Materials

Study Design and Patient Selection Criteria

The study was designed as a prospective observational study. Patients were selected for ICRS surgery with the following inclusion criteria: (1) stable keratoconus without any other ocular or systemic pathology affecting vision; (2) no prior cross-linking treatment; (3) insufficient spectacle corrected visual acuity to carry out daily tasks; (4) contact lens intolerance or impossibility to adapt contact lenses; (5) understanding of the limitations of the technique including the fact that contact lenses may be needed to achieve optimal visual acuity; and (6) ability to complete the follow-up. The study met the tenets of the Declaration of Helsinki. The study protocols were revised and approved by the Institutional Review Board of the Hospital Universitario Fundación Jiménez Díaz. Patients signed an informed consent prior to undertaking ICRS surgery.

Patients and Surgical Procedure

A total of 124 eyes (56 right eyes and 68 left eyes) from 96 patients (57 men and 39 women; 36 years old mean) were included in the study. A total of 172 segments were implanted. Ferrara Ring segments were implanted in 58 eyes (FerraraRing; AJL Ophthalmics, Vitoria, Spain) and Keraring segments were implanted in 66 eyes (KeraRing; Mediphacos, Belo Horizonte, Brazil).

Seven different ICRS combination were used as treatment for patients with keratoconus. The combination of segments was chosen according to the distribution of the curvature in the sagittal anterior map of the cornea following Keraring standard implantation guidelines (http://keraring.online).[18] Table 1 summarizes the keratoconic groups and their pre-operative profile.

All the surgeries were performed by the same corneal surgeon (N.A.). The ICRS surgery was performed with the patient under topical anesthesia. A tunnel channel was created using a 60-kHz infrared neodymium glass femtosecond laser at a wavelength of 1053 nm (IntraLase Inc., Irvine, CA). The intended tunnel depth was 80% of the thinnest point of the cornea with a maximum depth of 380 µm for segments

Table 1.   Pre-Operative Clinical Profile Description Segmented by Treatment Combination Cohorts

	Combination 1	Combination 2	Combination 3	Combination 4	Combination 5	Combination 6	Combination 7
Mean radius BFS (mm)	6.392 ± 0.327	6.468 ± 0.535	6.265 ± 0.67	6.601 ± 0.605	6.835 ± 0.63	6.578 ± 0.667	6.46 ± 0.825
Coma (μm)	1.358 ± 0.487	1.016 ± 0.589	1.008 ± 0.565	0.695 ± 0.376	1.029 ± 0.504	1.677 ± 1.227	1.231 ± 0.594
Corneal astigmatism (D)	6.233 ± 2.592	7.182 ± 1.736	5.029 ± 3.263	7.86 ± 2.601	4.634 ± 2.605	6.497 ± 3.1	4.102 ± 2.137
K_{max} (D)	58.598 ± 4.542	59.033 ± 3.894	60.774 ± 9.65	56.792 ± 5.601	54.551 ± 4.99	58.501 ± 7.663	59.591 ± 7.922
Sphere equivalent (D)	−4.521 ± 2.662	−9.341 ± 6.506	−9.006 ± 7.336	−7.688 ± 5.889	−5.016 ± 3.333	−4.948 ± 4.509	−5.964 ± 3.937
Cylinder (D)	−3.682 ± 1.031	−3.2 ± 2.683	−3.397 ± 1.775	−5.852 ± 2.125	−3.321 ± 1.007	−6.479 ± 1.866	−3.295 ± 2.395
Pre-operative BCVA	0.488 ± 0.216	0.497 ± 0.236	0.571 ± 0.19	0.627 ± 0.145	0.669 ± 0.202	0.408 ± 0.173	0.575 ± 0.246

Combination 1: Single 160 degrees segment. Combination 2: Two symmetrical 160 degrees segments. Combination 3: Single 210 degrees segment. Combination 4: Two symmetrical 120 degrees segments. Combination 5: Single 150 degrees segment. Combination 6: Two asymmetrical segments: 150 degrees inferior and 90 degrees superior. Combination 7: Single 210 degrees segment.

thinner than 300 μm and 400 μm for segments of 300 μm or larger, after marking a reference point in the pupil center. All patients received ofloxacin 4 times per day during 1 week and dexamethasone drops 4 times per day tapered every 5 days.

Clinical Examination

Pre-operative and postoperative evaluations were conducted 7 days before surgery and 3 months after surgery. The measurements included uncorrected visual acuity (UCVA) and best-corrected visual acuity (BCVA), manifest refraction, biomicroscopy, fundus evaluation, and corneal topography measurements (Pentacam, OCULUS Optikgeräte GmbH, Wetzlar, Germany). All measurements were performed with natural pupils under photopic conditions. Maximum elevation point given in diopters (K_{max}) by this device was collected both pre-operatively and postoperatively. BCVA was expressed in decimal units and obtained for the optimal monocular spherical and cylindrical correction. Spectacle refraction was transformed into spherical-equivalent and cartesian coordinates to perform vector analysis described by Alpins.[19] The anterior and posterior corneal topographies were obtained Pentacam by Oculus (25 cross-sectional Scheimpflug images; lateral resolution: 56.7 μm).

Three-Dimensional Surface Data Analysis and Retinal Image Quality Metrics

The commercial software of the Pentacam allowed the extraction of the raw elevation points of the corneal surfaces (anterior and posterior). The raw data consists of the elevation value for every corneal point sampled in 100-μm steps in a uniform square grid (from −7 to +7 mm, nasal-temporal, superior-inferior).

The corneal elevation data were fit by 3-D surfaces using custom routines written in Matlab (MathWorks, Natick, MA). The pupil center was taken, and not the corneal apex, was used as a reference in the aberration calculations, in both pre- and postoperative measurements. The pupil center defines the axis for vision, and therefore retinal image quality metrics from the wave aberration using this reference should better correlate vision. But, in addition, changes in the corneal vertex in keratoconus (with progression, and also pre- and postoperative) suggest that the pupil center is a preferable axis. The optical zone for data analysis was defined by the 4-mm diameter circular zone within the circumference defined by the ICRS radius (Fig. 1). Fits to a sphere, and biconicoids were used to obtain reference radii of curvature, asphericities and astigmatism. Data were extracted along the vertical and horizontal meridians as well as along the axis of the incision.

Anterior and posterior corneal elevation data (following subtraction of the best fitting sphere) were fitted by Zernike polynomial expansions (6th order) – note that these are fits to surface elevations not corneal wave aberrations. Zernike polynomials, have been used in numerous reports in the literature, including studies on keratoconus eye.[20] The corneal asymmetry was obtained using the root mean square (RMS) error of the asymmetric terms of the corneal elevation Zernike expansion (RMS_asym). RMS_asym was evaluated both including and excluding astigmatism coefficients, as previously described.[14] Corneal volume was estimated by computing the double integral over the corneal surfaces in the defined 4-mm diameter.

Corneal aberrations were computed for the central 4-mm pupil diameter area (within the ICRS) for the full cornea (anterior and poster surfaces), or the anterior cornea alone. The elevation data (in Zernike polynomial expansion) from both corneal surfaces were exported to ZEMAX (Focus Software, Tucson, AZ) for ray tracing analysis (performed at the corneal
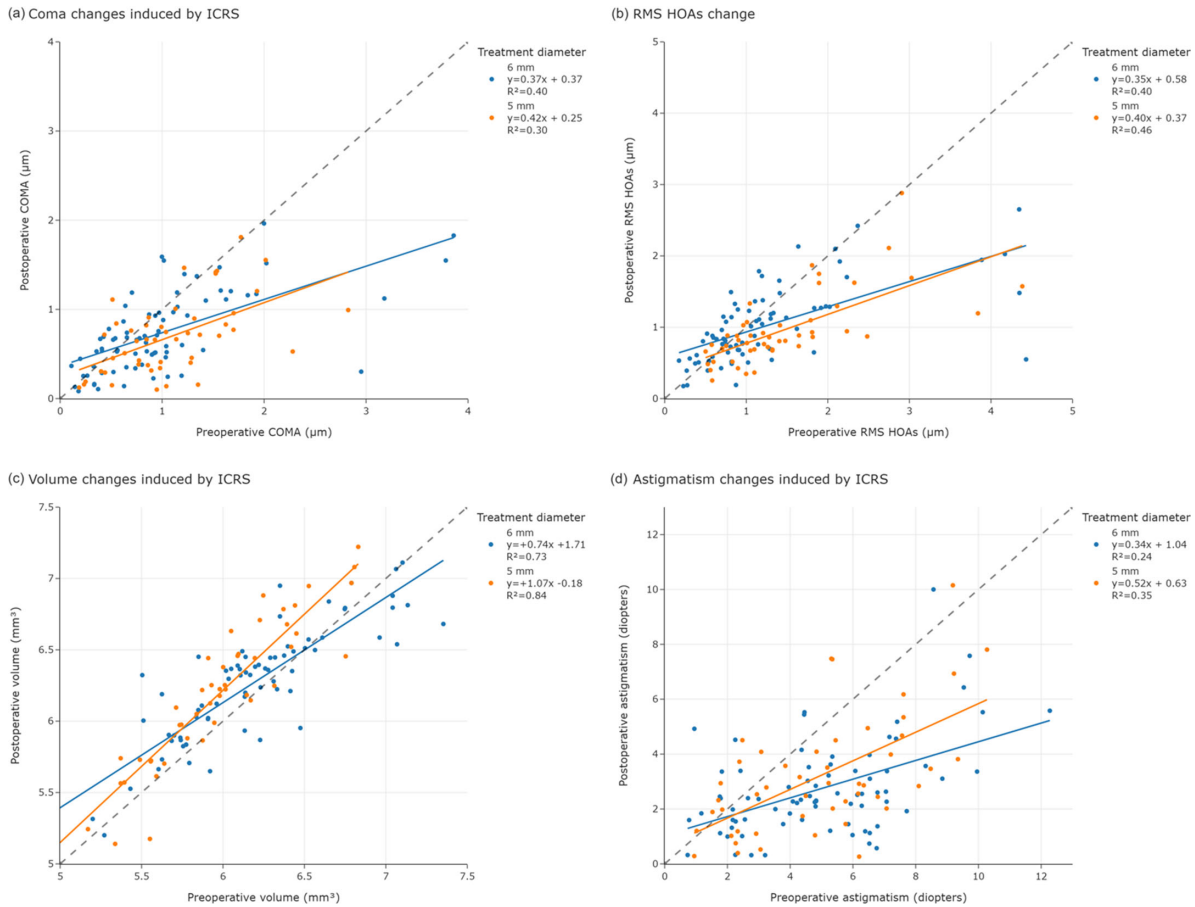
Figure 1. Main optical aberrations and corneal volume changes induced by intracorneal ring segments (ICRS) surgery implanted within 5 mm versus 6 mm of treatment diameter. Coma (a), high order aberrations (b), volume (c) and astigmatism (d) were computed considering both, anterior and posterior corneal surfaces and processed by a virtual ray tracing model.

focus). Refractive indices of 1.376 and 1.334 were used for the cornea and aqueous humour, respectively. Wave aberrations were calculated for monochromatic light (555 nm), by tracing an array of 64×64 collimated through a 1-surface (anterior cornea only) or 2-surface (anterior and posterior cornea, separated by corneal thickness) eye model. In the 1-surface model, the refractive index after the anterior corneal surface was set to 1.334. The contribution of the posterior corneal surface was obtained from direct subtraction of the anterior corneal surface aberrations from total corneal aberrations. Wave aberrations were described in terms of individual Zernike coefficients or RMS, in particular the RMS of astigmatism (RMS_astigmatism), the RMS of coma (RMS_coma). Retinal image quality was described in terms of the Visual Strehl (VS) metric. The VS ratio was computed as the volume under the Visual Module Transfer Function (VMTF; obtained from the overlapping of the module transfer function [MTF] with the inverse of a general Neural Transfer Function), normalized to diffraction limit.

VS was evaluated through focus (considering high order aberrations [HOAs] and cancelling the astigmatic terms). The maximum value of the through-focus VS curve was taken as the best corrected retinal image quality metric.[13]

Statistical Analysis

IBM SPSS Statistics 25.0 was used for the statistical analysis. Normal distribution of all data samples was first checked by means of Kolmogorov-Smirnov test. The relation between the VS (both with and without astigmatism) and BCVA was analyzed using the Pearson's Coefficient of correlation. The Spearman's coefficient was used to analyze the changes in several variables in relation with the depth of the segments and the width of the segments. Bonferroni correction was performed when evaluating geometric and aberrometric changes induced by different ICRS combinations.

Results

Pre-Operative Corneal Geometry

Treatment assignment according to Keraring standard guidelines showed some general tendencies related to pre-operative patient profile, represented in Table 1.

The 210 degree segments were implanted in those patients with steeper radius and high K_{max} values showing differences between groups in latter variable, the mean values were (6.53 ± 0.65 mm, $P = 0.08$) and (57.97 ± 6.94 D, $P = 0.022$), respectively. Asymmetrical segments disposition of 150 degrees inferior and 90 degrees superior were the treatment option when high amounts of coma and astigmatism were involved. Pre-operative coma was not comparable between groups ($P = 0.002$), range from 0.09 μm to 4.62 μm. Similarly, corneal astigmatism presented uneven groups distribution ($P < 0.001$) and wide range from 0.55 D to 14.71 D. The two symmetrical segments strategy (120 degrees or 160 degrees) was a suitable treatment option when low to moderate coma and high corneal astigmatism is shown. Refraction sphere-equivalent showed no differences among groups ($P = 0.19$).

Anterior Surface Corneal Geometry: Impact of ICRS on Radius of Curvature and Asphericity

On average, the cornea flattened postoperatively. The radius of curvature of the reference sphere increased significantly for both corneal surfaces in a 4-mm pupil diameter. ICRS showed more flattening effect on anterior corneal surface (+0.38 mm, 5.8%, $P < 0.001$) in comparison with its impact on the posterior corneal surface (+0.15 mm, 3.14%, $P < 0.001$). The K_{max} changed from 57.97 ± 6.9 D to 55.39 ± 6.1 D (−2.58 D, 4.83%, $P < 0.001$). Anterior corneal asphericity shifted to more negative values, although the change was only significant for 6-mm segments (from −1.23 ± 1.1 to −1.86 ± 1.2, $P < 0.001$), whereas the change in asphericity induced by 5-mm segments was not statistically significant (from −1.99 ± 1.1 to −2.10 ± 1.5, $P = 0.536$). Table 2 shows the geometrical changes of the anterior cornea after the ICRS surgery.

Posterior Surface Corneal Geometry: Impact of ICRS on Radius of Curvature and Asphericity

On average, there was also a flattening of the posterior surface while its asphericity remained stable. In all cases, the curvature changes in the posterior surface paralleled the changes of the anterior surface. As an example, the 6 mm 120 degrees/120 degrees combination flattened the anterior surface of the steepest axis (+0.33 mm) and the posterior surface is also flattened in the same meridian (+0.28 mm, $P < 0.001$) but showed steepening in both surfaces in the flattest meridian (−0.35 mm anterior, −0.54 mm posterior, $P < 0.001$).

Corneal Asymmetry of the Anterior and Posterior Corneal Surfaces After ICRS Surgery

Anterior surface RMS_asym decreased significantly (from 4.2 ± 1.2 μm to 3.1 ± 1.2 μm, $P < 0.001$). There was also a trend for posterior surface RMS_asym decrease, but it was not statistically significant ($P = 0.416$). Globally, these trend in RMS_asym were similar for 5-mm (48 patients with RMS_asym changed from 4.7 ± 1.8 μm to 3.9 ± 1.9 μm, $P < 0.001$) and 6-mm ICRS optical zones (76 patients with RMS_asym changed from 4.5 ± 2.3 μm to 3.3 ± 2.9 μm, $P = 0.069$) but in the second group the variability was larger, and the change did not reach statistical significance. Coma and RMS_HOA changes are detailed in Figure 1A and Figure 1B, respectively.

Table 2. Both Corneal Surfaces Pre and Postoperative Main Values and Geometrical Changes Caused by ISCRS Surgery

Corneal Surface	Variable	N	Pre-Operative	Post-Operative	Change	P Value
Anterior surface	**K max (D)**	124	57.97 ± 6.94	55.39 ± 6.10	−2.58 (−3.08, −2.07)	<0.001
	Mean radius BFS (mm)	124	6.53 ± 0.64	6.91 ± 0.63	0.38 (0.32, 0.43)	<0.001
	Asphericity	124	−1.53 ± 1.12	−1.96 ± 1.36	−0.43 (−0.63, −0.22)	<0.001
Posterior surface	**Mean radius BFS (mm)**	124	4.97 ± 0.70	5.124 ± 0.67	0.156 (0.109, 0.204)	<0.001
	Asphericity	124	−1.57 ± 1.10	−1.64 ± 1.16	−0.062 (−0.211, 0.087)	0.409

N, sample size; BFS, best fitting sphere.

Corneal Volume After ICRS Surgery

Corneal volume (in the central zone, 4-mm) increased statistically significantly (0.094 mm^3, $P < 0.005$; pre-operative $= 6.13 \pm 0.56$ mm^3, and postoperative $= 6.23 \pm 0.48$ mm^3), both for 5-mm ICRS optical zone (0.147 mm^3, $P = 0.046$; pre-operative $= 6.03 \pm 0.59$ mm^3, and postoperative $= 6.18 \pm 0.52$ mm^3) and in 6-mm ICRS optical zone (0.062 mm^3, $P = 0.042$; pre-operative $= 6.19 \pm 0.53$ mm^3, and postoperative $= 6.26 \pm 0.45$ mm^3). Figure 1C illustrates corneal volume changes.

Visual Quality After ICRS Surgery: Astigmatism and High-Order Aberrations

Corneal aberrations (considering the anterior and posterior corneal surfaces) decreased significantly 3 months after ICRS implantation: RMS_HOA by 0.33 µm ($P < 0.001$, 24.8% decrease), RMS_coma decreased by 0.31 µm ($P < 0.001$, 30.12%). Corneal wavefront astigmatism decreased by 2.05 D ($P < 0.001$, 41.2%). Trefoil did not change significantly with surgery. VS for astigmatism and HOAs increased significantly ($P < 0.001$). Figure 1D shows the collect corneal astigmatism changes and Table 3 shows the aberrometry and the visual changes after the ICRS surgery.

Subjective Refraction and Visual Acuity After ICRS Implantation

Clinically, the improvement on retinal image quality was associated with a decrease in the spherical equivalent by 2.43 D (from -6.71 to -4.28, 36.23%, $P < 0.001$) and a decrease in subjective astigmatism by 2.26 D (from -4.31 to -2.05, 52.63%, $P < 0.001$). The studied patients experienced an improvement in BCVA

of more than one line (23%, $P < 0.001$). Fourteen patients out of 124 patients (11.3%) experienced a decrease in BCVA (see Table 3).

Impact on Corneal Geometry and Aberrations of Different ICRS Combinations

Figure 2 represents changes produced by each segment combination classified by diameter treatment, analyzing the impact in coma, RMS_HOA, astigmatism, and VS of HOAs. Table 4 summarizes the main changes induced by each combination of segments.

−5 mm-Optical Zone ICRS

Combination 1: **Single 160-Degree Segment (12 Eyes)**
This segment produced flattening of the anterior surface of the cornea (both reference sphere and K$_{max}$). It reduced corneal aberrations targeting very specifically coma and had a significant impact on astigmatism, improving BCVA (from 0.488 ± 0.216 to 0.633 ± 0.187, $P = 0.046$). Despite a relatively low number of patients in this group, changes are significant and showed a statistically significant decrease in RMS_asym for both the anterior surface of the cornea (from 4.3 ± 1.5 µm to 3.2 ± 1.4 µm, $P = 0.003$) and the posterior surface of the cornea (from 9.7 ± 2.9 µm to 8.7 ± 2.6 µm, $P = 0.044$).

Combination 2: **Two Symmetrical 160-Degree Segments (12 Eyes)**
This combination of ICRS produced the largest flattening in the anterior surface (both reference sphere and K$_{max}$). As expected, given the symmetrical combination of ICRS, the impact on coma was smaller than in asymmetrical combinations. BCVA improved significantly (from 0.49 ± 0.23 to 0.65 ± 0.28, $P = 0.004$)

Table 3. Monochromatic Optical Aberrations Grouped by Class and Visual Performance Before and After ISCRS Surgery

	N	Pre	Post	Change	*P*-Value
RMS HOAs (µm)	124	1.32 ± 0.91	0.99 ± 0.52	-0.33 (-0.453, -0.202)	<0.001
Coma (µm)	124	1.03 ± 0.67	0.72 ± 0.43	-0.31 (-0.407, -0.214)	<0.001
Trefoil (µm)	124	0.29 ± 0.26	0.32 ± 0.25	0.024 (-0.035, 0.083)	0.418
Astigmatism (µm)	124	-4.97 ± 2.46	-2.92 ± 1.91	2.05 (1.661, 2.437)	<0.001
Visual Strehl	124	0.049 ± 0.02	0.065 ± 0.041	0.016 (0.011, 0.022)	<0.001
BCVA	124	0.57 ± 0.21	0.69 ± 0.21	0.125 (0.091, 0.159)	<0.001
Refractive sphere (D)	124	-6.71 ± 5.41	-4.28 ± 4.09	2.434 (1.739, 3.130)	<0.001
Refractive cylinder (D)	124	-4.31 ± 2.18	-2.05 ± 1.55	2.263 (1.773, 2.753)	<0.001

N, sample size; RMS HOAs, root mean square of the high-order aberrations (µm); coma (µm); trefoil (µm); astigmatism (D); BCVA, best-corrected visual acuity; subjective refraction: sphere and cylinder (D).
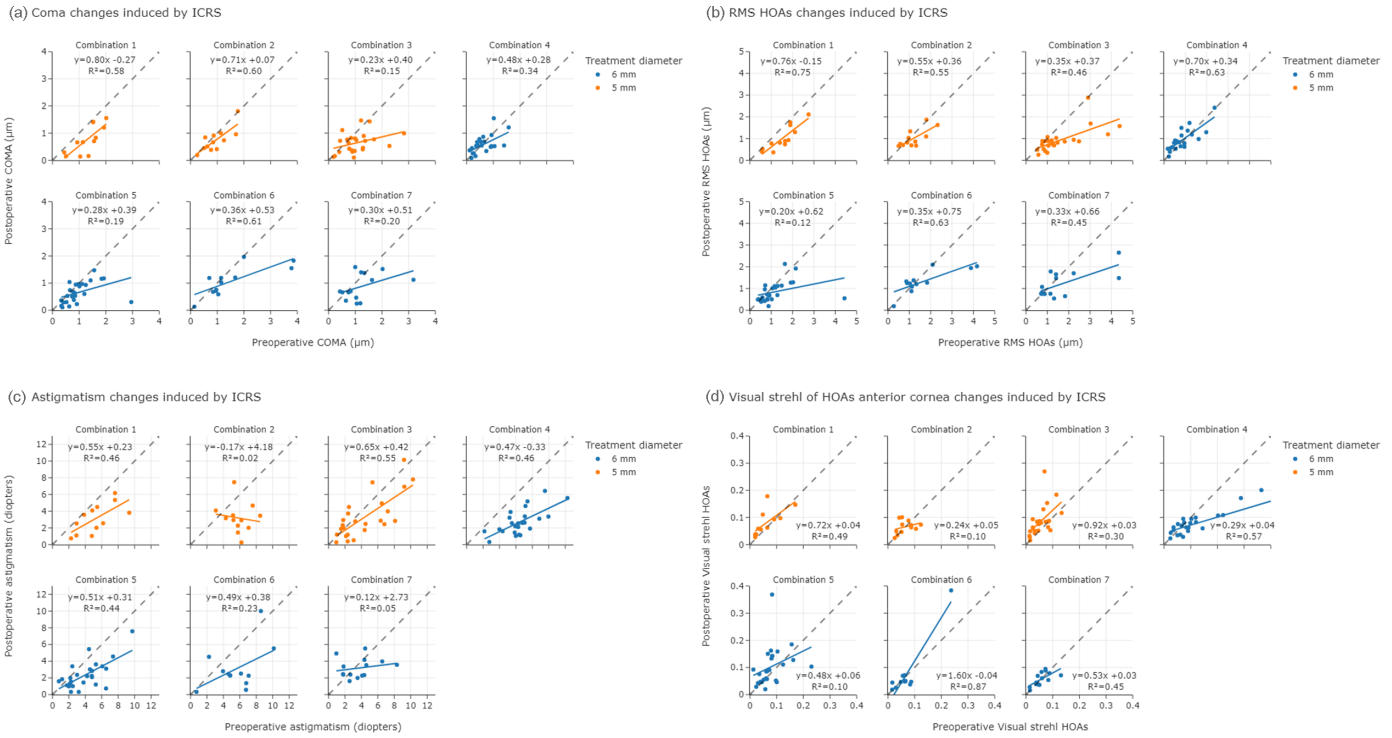
Figure 2. Pre- and postoperative coma (a), high order aberrations (b), astigmatism (c), and Visual Strehl (d) comparison for each combination of intracorneal rings segments (ICRS). Combination 1: single 160 degrees, combination 2: two symmetrical 160 degrees, combination 3: single 210, combination 4: two symmetrical 120 degrees, combination 5: single 150 degrees, combination 6: 150 degrees superior and 90 degrees inferior, combination 7: single 210 degrees.

Table 4. Geometrical and Aberrometric Changes After ICRS Surgery Induced by Each Combination of ICRS

	Combination 1	Combination 2	Combination 3	Combination 4	Combination 5	Combination 6	Combination 7
R (mm)	0.45 ± 0.286**	0.638 ± 0.256*	0.539 ± 0.309*	0.165 ± 0.133*	0.293 ± 0.232*	0.333 ± 0.536	0.383 ± 0.186*
R ICRS meridian (mm)	0.494 ± 0.338**	0.571 ± 0.429**	0.514 ± 0.298*	-0.351 ± 0.293*	0.273 ± 0.298**	0.214 ± 0.575	0.143 ± 0.452
R ICRS perpendicular meridian (mm)	0.511 ± 0.508	0.446 ± 0.454	0.558 ± 0.529**	0.334 ± 0.309*	0.199 ± 0.437	0.191 ± 0.714	0.320 ± 0.560
K max (D)	-3.38 ± 2.355**	-4.78 ± 2.142*	-3.92 ± 3.269*	-1.91 ± 1.441*	-1.39 ± 2.708	-2.32 ± 2.864	-1.25 ± 3.291
Asphericity	0.325 ± 0.774	-0.67 ± 1.455	-0.046 ± 1.226	-0.75 ± 0.682*	-0.344 ± 0.784	-0.58 ± 1.047	-0.99 ± 1.793
Asphericity ICRS meridian	1.036 ± 1.722	-0.78 ± 2.057	-0.093 ± 1.075	-0.99 ± 1.170**	-0.301 ± 0.972	-0.73 ± 1.101	-1.17 ± 1.941
Asphericity ICRS perpendicular meridian	-0.154 ± 1.416	-1.16 ± 1.434	-0.396 ± 1.977	-0.379 ± 1.012	-0.170 ± 2.003	-0.96 ± 2.344	-0.85 ± 2.676
RMS (µm)	-0.52 ± 0.316**	-0.184 ± 0.367	-0.66 ± 0.780**	0.085 ± 0.333	-0.318 ± 0.791	-0.184 ± 0.367	-0.441 ± 0.936
Coma (µm)	-0.53 ± 0.356**	-0.201 ± 0.298	-0.415 ± 0.579	-0.050 ± 0.331	-0.323 ± 0.544	-0.201 ± 0.298	-0.336 ± 0.657
Wavefront Astigmatism (D)	2.136 ± 1.611**	2.658 ± 2.449	1.091 ± 1.998	3.788 ± 1.628*	1.635 ± 1.607*	2.658 ± 2.449	0.518 ± 2.100
Visual Strehl	0.026 ± 0.022	0.008 ± 0.016	0.021 ± 0.032	0.021 ± 0.018*	0.021 ± 0.039	0.008 ± 0.016	-0.009 ± 0.035
Spherical Equivalent (D)	0.271 ± 2.913	6.341 ± 4.141**	3.262 ± 4.342	2.551 ± 4.328	1.130 ± 2.368	6.341 ± 4.141**	2.295 ± 2.745
Refractive Astigmatism (D)	1.409 ± 0.976**	0.700 ± 2.280	0.868 ± 1.814	4.216 ± 2.419*	1.810 ± 1.396*	4.375 ± 2.018*	0.636 ± 2.782
Refractive SIA (D)	2.685 ± 1.409**	4.231 ± 2.493**	3.025 ± 2.177*	6.334 ± 2.447*	3.103 ± 1.812*	6.156 ± 2.420*	2.749 ± 2.293**

*$p < 0.001$, **$p < 0.05$.

R (mm)/asph, radius of curvature and asphericity of the anterior cornea (conic fitting); R (mm)/asph ICRS meridian, radius of curvature and asphericity of the anterior cornea in the meridian of the segment; R (mm)/asph ICRS perpendicular meridian, radius of curvature and asphericity of the anterior cornea in the perpendicular of the meridian of the segment; wavefront astigmatism (D); spherical equivalent (D); refractive astigmatism (D); SIA (D), surgically induced astigmatism.

and showed a clear trend to improvement in VS. This combination showed no impact in the RMS of the surfaces of the cornea.

***Combination 3:* Single 210-Degree Segments (24 Eyes)**

This combination of ICRS induced a significant flattening (both reference sphere and K_{max}) and reduced corneal aberrations, although the impact on aberrations and refractive astigmatism was relatively small (even if the spectacle cylindrical change was bigger than expected). These ICRS segments decreased the RMS of the anterior surface (from 3.7 ± 1.4 µm to 2.7 ± 1.4 µm, $P = 0.015$) but not the RMS of the posterior surface.

−6 mm-Optical Zone ICRS

Combination 4: Two Symmetrical 120-Degree Segments (24 Eyes)

This combination of ICRS highly reduced astigmatism (from -6.51 ± 2.2 to -2.73 ± 1.5 D, $P < 0.001$), although only produced a modest corneal flattening of the cornea even if statistically significant (from 6.61 ± 0.6 to 6.76 ± 0.6 mm, $P < 0.001$). It did not have impact on corneal aberrations.

Interestingly, in a subgroup of patients with preoperative coma over 0.7 μm, segments were placed closer to each other in their inferior end, which resulted in a decrease of coma RMS from 1.05 ± 0.26 μm preoperatively to 0.73 ± 0.41 μm postoperatively (30.49% decrease, $P = 0.039$). This decreased in coma had a significant effect on VS (which increased from 0.042 ± 0.016 to 0.064 ± 0.028, $P < 0.001$) but not on BCVA.

Two patient lost four lines of BCVA, paralleling an increase of refractive defocus and astigmatism, and of high order aberrations (in particular, coma). In fact, this combination showed a statistically significant increase in the asymmetry of both the anterior surface of the cornea (RMS_asym changed from 2.2 ± 0.8 μm to 2.6 ± 1.1 μm, $P < 0.005$) and of the posterior surface of the cornea (RMS_asym went from 5.3 ± 2.4 μm to 6.4 ± 2.5 μm, $P < 0.018$) with an increase in the trefoil (from 0.211 ± 0.166 μm to 0.388 ± 0.266 μm, $P = 0.003$).

Combination 5: Single 150-Degree Segments (26 Eyes)

This combination ICRS flattened the anterior surface of the cornea specially on the sphere reference analysis; it also reduced corneal aberrations targeting very specifically coma and had a significant impact on astigmatism, improving BCVA (from 0.669 ± 0.202 to 0.787 ± 0.170, $P < 0.001$), VS is positively affected by this combination, even though the change produced did not reach statistical threshold.

Combination 6: Two Asymmetrical Segments: 150 Degrees Inferior and 90 Degrees Superior (12 Eyes)

This combination of ICRS produced a moderate flattening of the cornea ($K_{max} = 58.5 \pm 7.6$ D preoperative; 56.1 ± 5.9 D postoperative; $P = 0.669$), a highly statistically significant reduction of refractive astigmatism (from -5.55 ± 2.5 to -2.35 ± 1.6 D; $P = 0.123$) and a slight decrease in coma, although not statistically significantly (from 1.52 ± 1.1 to 1.06 ± 0.5 μm; $P = 1.00$).

Combination 7: Single 210-Degree Segment (14 Eyes)

The flattening of the cornea with these segments was modest, even statistically significant in the reference sphere. Moreover, in 6 patients, the value of K_{max} decreased less than 1 D, while it showed an increased in 4 of them. The effect on aberrations and astigmatism was also not statistically significant. Three patients lost BCVA, in two of them, the segment failed to flatten the cornea. Notably, the VS worsened in this group (not statistically significant). There was no impact of these segments in the RMS of both surfaces of the cornea.

5-mm versus 6-mm Optical Diameter

As previously reported,[13] we found that ICRSs implanted in a 5 mm-optical diameter zone produced a statistically higher flattening of the cornea and larger improvement in retinal image quality than 6 mm-optical diameter segments. Table 5 compares the effect of 150 degrees to 6 mm segments (24 patients) versus 160 degrees to 5 mm segments (12 patients) and the effect of 210 degrees to 6 mm segments (12 patients) versus 210 degrees to 5 mm segments (24 patients) on the corneal elevation maps and the corneal wavefront aberrations (4-mm diameter). Differences are not significant for astigmatism.

We found a weak correlation between ICRS width and corneal flattening ($r = 0.27$, $P = 0.007$). In addition, for the ICRS 5 mm 210 degree segments, we found a statistically significant correlation between the width and reduction of the coma ($r = 0.49$,

Table 5. Geometric and Visual Differences Between Different Optical Zones for the 160–150 Segments and 210 Segments

	6–150	5–160	P Value	6–210	5–210	P Value
K max (D)	-1.39 ± 2.71	-3.38 ± 2.35	0.035	-1.25 ± 3.29	-3.92 ± 3.27	0.021
Mean radius BFS (mm)	0.29 ± 0.23	0.45 ± 0.28	0.077	0.38 ± 0.18	0.54 ± 0.31	0.096
Coma (μm)	-0.32 ± 0.54	-0.53 ± 0.35	0.227	-0.33 ± 0.65	-0.41 ± 0.58	0.703
Astigmatism	-1.63 ± 1.61	-2.13 ± 1.61	0.377	0.51 ± 2.10	1.09 ± 1.99	0.408
Visual Strehl	0.021 ± 0.04	0.02 ± 0.02	0.636	-0.009 ± 0.035	0.021 ± 0.032	0.009

$P = 0.03$). The statistical power is in part reduced (despite the relatively large sample) by the ICRS thickness as a covariable (and generally associated to the severity of the keratoconus, which tends to be treated with wider ICRS).

Discussion

The present study targeted the evaluation of the corneal and clinical changes induced by insertion of ICRS in patients with keratoconus. We chose a follow-up timeframe of 3 months for various reasons: (i) there is a consensus that the effect produced by the ICRS is stable around 3 months after surgery[21–23]; (ii) we wanted to avoid a possible progression of the disease to interfere with the results, which may have occurred with longer follow-up[22]; and (iii) the reported potential migration of the segments along time is possible and should be minimized over a relative short period of time and therefore excluded as a confounding variable. As in our previous study, the choice of a 4 mm pupil allows targeting the optical zone inside the segments, avoiding the measurement distortions introduced by the segment itself.[13]

In our study, the curvature of the best fitting spherical surface (4 mm) shifted from 57.55 D to 54.39 D (assuming an index of refraction of 1.376 in the radius to curvature transformation) or from 51.65 ± 4.65 D to 48.82 ± 4.06 D (assuming the keratometric index of refraction used by most of the topographers 1.3375). These changes are similar to other studies implanting triangular section ICRS. Average changes in K_{max} are also consistent with those found in previous studies (from 57.97 ± 6.94 D to 55.39 ± 6.10 D, index of refraction 1.3375).

Our analysis expands that of previous studies of keratometric changes in the cornea following ICRS implantation. Given the general asymmetric nature of the corneal topography in keratoconus, and the non-rotationally symmetric implantation of ICRS, the use of biconicoids, and high order Zernike terms appears best suited for the analysis. Biomechanical models[8,24] predict that the effect of the segments is largest in the vicinity of the segments and it is reduced away from their location. A similar observation was also made on ICRS implants in donor eyes from eye banks.[25] The relative difference in flattening in the center/periphery produces changes in the asphericity, in principle, consistent with a negative asphericity within the central 4 mm, especially if 6 mm segments are used. We found corneal asphericity (Q) shifts from -1.53 to -1.96 from conicoid fit. The same trend was found

in all studied meridians (the steepest axis, the flattest axis, the axis of the coma, and the axis perpendicular to the coma axis). In contrast, Torquetti et al.[26] found a decrease in the magnitude of asphericity after ICRS implantation, with Q values shifting from -1.23 to -0.41, although there appears to be a large variability in the asphericity estimates.[27] We hypothesize that the trend in their study may be associated to their nomogram (as they indicate the use of longer arc length segments and a decrease in corneal asphericity as a target, even if they failed to show statistical differences associated to the arc length). Additional potential reasons for the discrepancy may be the choice of an 8-mm fitting area, and a potential instrument bias of using the Galilei for this purpose.[26] Incidentally, Utine et al.[28] using Pentacam found a similar change in asphericity after ICRS implantation as the one we report.

After ICRS implantation following the manufacturer's guidelines approach, we found a statistically significant reduction in high order aberrations, coma and wavefront astigmatism, more pronounced than in other studies. For example, previous studies by Piñero et al.[29] and Shabayek et al.[15] failed at finding a statistically significant reduction in RMS_HOA or RMS_coma and found a small statistically significant decrease in RMS_astigmatism.

Our dedicated analysis integrated a large range of keratoconus and of a combination of segments and therefore a strict comparison of aberrometry with prior reports should not be attempted, as generally those studies limit the population to those within certain values of astigmatism and/or coma orientations. Prior published studies did not customize the arc of the implanted segments according to the topography of the patient. Classical nomograms[30–32] choose the steepest axis to implant two segments with the same arc length that sometimes differ in thickness, and generally only consider spherical equivalent, astigmatism, and qualitative asymmetry of the axial map of the anterior surface of the cornea in their nomograms for ICRS selection. Our results suggest that a more personalized approach leads to better aberrometric results. More recent studies using a more personalized approach, such as that proposed by Torquetti et al.,[26] did find a significant reduction in both RMS_HOA and RMS_coma using a 6 mm pupil size. Unlike our approach, they only considered the topographic astigmatism and the location of the ectasia to choose the segments and based their approach in a nomogram dated in 2009.[33]

In addition, it has been reported that VS is a good optical predictor of visual acuity.[34] In our study, we found a good correlation between VS and BCVA

pre-operatively, but not postoperatively. This discrepancy may be due to various factors: (i) BCVA may not be a sufficiently sensitive metric; (ii) several patients experienced dramatic improvements in their astigmatism without changing or even with a slight decrease in BCVA. This improvement in their astigmatism will be accompanied by an improvement in their VS and by a reduction in the correlation between BCVA and VS; (iii) likely prior adaptation to the native high order aberrations, and specifically astigmatism; and (iv) BCVA may be failing at capturing the shifts in perceived best focus that are better captured using perceived visual quality judgments. Sabesan et al.[35] concluded that the patients with keratoconus are in fact adapted to their aberrations, as normal patients are imposed with similar aberration patterns/magnitudes using adaptive optics performed visually poorer than true keratoconus (despite the retinal image quality being identical in both groups). In addition, patients with keratoconus can be trained to improve their maximum BCVA if their retinal image quality is improved.[36] On the other hand, Sawides et al.[37] found that subjects rapidly recalibrated to increased/decreased aberration magnitudes, using perceived visual judgments as a metric. In a subsequent study, these authors found that eyes adapt to changes in blurred orientation, and, in fact, patients with astigmatism are adapted to the orientation of blur produced by their own astigmatism.[38] A dynamic recalibration to the presence of astigmatism is supported by the fact that the perceived isotropic focus shifted toward isotropy in astigmatic patients (normally uncorrected) fairly rapidly after correction of their astigmatism. Vinas et al. showed rapid changes in the best perceived focus following clinical correction of astigmatism,[39] however, the bias toward the orientation of their native blur still persisted at least 6 months after astigmatism correction in visual acuity metrics.[40] In fact, former patients with astigmatism were more insensitive (visual acuity was less degraded) by the induction of astigmatism than non-astigmats. These results may be extrapolated to the ICRS-implanted patients, although systematic studies reporting VS, visual acuity, and perceived visual quality before and after ICRS implantation are pending.

In addition, in our cohort, some patients experienced important improvements in BCVA with slight improvements in VS. We can speculate potential explanations for this effect. We have previously published that the patients with keratoconus frequently present signs and symptoms of dry eye disease and also that they improve after ICRS implantation.[41] It is possible that the tear film stabilization leads to an improvement in BCVA. In addition, patients with keratoconus may recalibrate faster to a new aberration pattern than a normal population.[35] It may be possible that a small improvement in the quality of the images can lead to a great change in BCVA in some patients because of their neural adaptation.[36]

The changes induced by ICRS significantly improved the refraction of the patients. There was a significant decrease in the spherical equivalent and the refractive astigmatism was reduced by over half. These changes in astigmatism are also larger than in other reported series of patients,[4] probably due to the higher customization in our study. All those changes led to a statistically significant improvement in BCVA. However, 11.29% (14 out of 124 patients) of the patients lost BCVA. A loss in BCVA does not directly imply an unsuccessful outcome in this population. Six (42.9%) of those 14 patients were implanted with two 120 degree segments; that combination is used mainly in very high regular astigmatism. For example, a patient with BCVA of 0.9 with a 6 D measured astigmatism, left uncorrected due to intolerance to the astigmatic correction. After surgery, astigmatism improved (2 D) but BCVA decreased to 0.7. In other patients, the indication of ICRS insertion was made not to improve BCVA but to improve contact lens fitting, which was aided by the significant corneal flattening.

The changes obtained with each combination of segments can be observed in Table 4. Globally, 6-mm optical diameter ICRS appear to be very effective in reducing astigmatism, flatten the cornea, and improve aberrations. However, 5-mm optical zone ICRS induce a larger flattening and are more effective in reducing aberrations.

Shorter segments seem less effective in producing flattening and reducing aberrations than larger segments but more effective in reducing astigmatism. Symmetrical implants are very good at reducing astigmatism but show very small impact on high order aberrations. A displacement of the ICRS, so that they are near each other in the steepest corneal region (if the cornea is asymmetric), significantly reduces coma.

In asymmetrical corneas, adding a superior segment with short arc length produces larger astigmatism correction. Other studies have analyzed specific combination of segments. For example, a study from Sandes et al.[42] evaluated the performance of 140 degrees 5 mm-ICRS. Group 2 and group 3 in that study (30 and 11 eyes) received an implant of one segment of 150 and 200 microns, respectively. They showed a decrease in tomographic astigmatism of 2.5 D (39.68%) and 3.8 D (50.76%), not far from the changes that we found in the aberrometric astigmatism with one 5-mm 160-degree segments. They did not study neither K_{max} nor corneal

aberrations or subjective refraction. In addition, the patients in that study exhibited much higher astigmatism. The differences in the patient profiles and implants prevent us from a direct comparison. Lisa et al.[43] presented similar results with these segments in a group of patients with similar characteristics. Our cohort included patients with higher K_{max} values (60.77 D against 53.89 D), which may explain the larger induced flattening in our patients compared to the prior study (−3.92 D 6.45%, against −2.62 D 4.86%), likely as a result of wider ICRS in our study (there was no description of the specifications used in their work). Similarly, the spherical equivalent in our group was much larger (−9.01 D) than in their study (−3.19 D) showing a larger reduction. The change in the refractive cylinder was similar in both studies. They also reported negative asphericity, although this corresponded to an 8-mm diameter fit. As mentioned, an applanation in the central cornea is likely to lead to a decrease in asphericity for a larger area. In our group, the change in asphericity measured at 4 mm was not statistically significant. This combination, however, may be a good choice if an increase in the asphericity is not desired.

We also analyzed the extent to which the planned width of the ICRS influenced the postoperative outcomes. As expected, there was a trend for the effect of the ICRS to be larger with wider segments, but the correlation was disappointingly weak. These results are somehow surprising because previous work found significant correlations between the width of the segments and the induced changes. The group of Ferrara (adapted from Ref. 44) even proposed a precise nomogram for the 160 degrees 5 mm segments based on those observations. The poor predictability on the effect of the width of segments in the outcomes could be explained by the fact that wider segments are normally placed in more advanced keratoconus. Histological studies have shown a progressive corneal thinning in more advanced keratoconus along with altered structure in the area of the cornea. Biomechanical studies have shown a relation between loss of structure and mechanical weakening and predict a smaller effect of ICRS in weaker corneas than in stiffer corneas, which may bias the effect of the width of the segments, given the interactions between the magnitude of the intended effect and corneal weakness.[8]

To summarize, anterior and posterior corneal topography in combination with custom routines for the analysis of irregular corneas have allowed a comprehensive evaluation of optical and corneal changes induced by different combinations of ICRS in keratoconic eyes. We found that: (i) ICRS increases the volume in the area between them, and (ii) 5 mm segments are more effective in flattening the cornea and asymmetric implants in regularizing it, whereas 6 mm segments are as effective in reducing astigmatism and are a good choice if the asymmetry and the intended flattening are smaller. Further analysis should incorporate not only morphological but also biomechanical properties to produce more accurate nomograms for ICRS surgical planning and increase the predictability of ICRS surgery.

Disclosure: **N. Alejandre,** None; **P. Pérez-Merino,** None; **G. Velarde,** None; **I. Jiménez-Alfaro,** None; **S. Marcos,** None

References

1. Nordan LT. Keratoconus: Diagnosis and treatment. *Int Ophthalmol Clin*. 1997;37(1):51–63.
2. Rabinowitz YS. Keratoconus. *Surv Ophthalmol*. 1998;42(4):297–319.
3. Piñero DP, Alio JL, Kady B El, et al. Refractive and Aberrometric Outcomes of Intracorneal Ring Segments for Keratoconus: Mechanical versus Femtosecond-assisted Procedures. *Ophthalmology*. 2009;116(9):1675–1687.
4. Peña-García P, Alió JL, Vega-Estrada A, Barraquer RI. Internal, corneal, and refractive astigmatism as prognostic factors for intrastromal corneal ring segment implantation in mild to moderate keratoconus. *J Cataract Refract Surg*. 2014;40(10):1633–1644.
5. Peña-García P, Vega-Estrada A, Barraquer RI, Burguera-Giménez N, Alio JL. Intracorneal ring segment in keratoconus: A model to predict visual changes induced by the surgery. *Investig Ophthalmol Vis Sci*. 2012;53(13):8447–8457.
6. Torquetti L, Ferrara G, Almeida F, et al. Intrastromal corneal ring segments implantation in patients with keratoconus: 10-year follow-up. *J Refract Surg*. 2014;30(1):22–26.
7. Giacomin NT, Mello GR, Medeiros CS, et al. Intracorneal ring segments implantation for corneal ectasia. *J Refract Surg*. 2016;32(12):829–839.

8. Kling S, Marcos S. Finite-element modeling of intrastromal ring segment implantation into a hyperelastic cornea. *Investig Ophthalmol Vis Sci*. 2013;54(1):881–889.

9. Roberts CJ, Dupps WJ. Biomechanics of corneal ectasia and biomechanical treatments. *J Cataract Refract Surg*. 2014;40(6):991–998.

10. Dauwe C, Touboul D, Roberts CJ, et al. Biomechanical and morphological corneal response to placement of intrastromal corneal ring segments for keratoconus. *J Cataract Refract Surg*. 2009;35(10):1761–1767.

11. Torquetti L, Ferrara P. Intrastromal corneal ring segment implantation for ectasia after refractive surgery. *J Cataract Refract Surg*. 2010;36(6):986–990.

12. Ortiz S, Pérez-Merino P, Alejandre N, Gambra E, Jimenez-Alfaro I, Marcos S. Quantitative OCT-based corneal topography in keratoconus with intracorneal ring segments. *Biomed Opt Express*. 2012;3(5):814.

13. Pérez-Merino P, Ortiz S, Alejandre N, De Castro A, Jiménez-Alfaro I, Marcos S. Ocular and optical coherence tomography-based corneal aberrometry in keratoconic eyes treated by intracorneal ring segments. *Am J Ophthalmol*. 2014;157(1):116–127.

14. Pérez-Merino P, Ortiz S, Alejandre N, Jiménez-Alfaro I, Marcos S. Quantitative OCT-based longitudinal evaluation of intracorneal ring segment implantation in keratoconus. *Investig Ophthalmol Vis Sci*. 2013;54(9):6040–6051.

15. Shabayek MH, Alió JL. Intrastromal Corneal Ring Segment Implantation by Femtosecond Laser for Keratoconus Correction. *Ophthalmology*. 2007;114(9):1643–1652.

16. Söğütlü E, Piñero DP, Kubaloglu A, Alio JL, Cinar Y. Elevation changes of central posterior corneal surface after intracorneal ring segment implantation in keratoconus. *Cornea*. 2012;31(4):387–395.

17. Piñero DP, Alio JL, Teus MA, Barraquer RI, Uceda-Montañés A. Modeling the intracorneal ring segment effect in keratoconus using refractive, Keratometric, and corneal aberrometric data. *Investig Ophthalmol Vis Sci*. 2010;51(11):5583–5591.

18. Keraring on line. Philosophy of Keraring surgical planning. Available at: http://keraring.online.

19. Alpins N. Astigmatism analysis by the Alpins method. *J Cataract Refract Surg*. 2001;27(1):31–49.

20. Barbero S, Marcos S, Merayo-Lloves J, Moreno-Barriuso E. Validation of the estimation of corneal aberrations from videokeratography in keratoconus. *J Refract Surg*. 2002;18(3):263–270.

21. Wijdh RH, van Rij G. Intrastromal Corneal Ring Segments (ICRS): Three- and six months results. *Documenta Ophthalmologica*. Vol 100. Doc Ophthalmol; 2000;100(1):27–37.

22. Vega-Estrada A, Alió JL, Plaza-Puche AB. Keratoconus progression after intrastromal corneal ring segment implantation in young patients: Five-year follow-up. *J Cataract Refract Surg*. 2015;41(6):1145–1152.

23. Pérez-Merino P, Parra F, Ibares-Frías L, et al. Clinical and pathological effects of different acrylic intracorneal ring segments in corneal additive surgery. *Acta Biomater*. 2010;6(7):2572–2579.

24. Lago MA, Rupérez MJ, Monserrat C, et al. Patient-specific simulation of the intrastromal ring segment implantation in corneas with keratoconus. *J Mech Behav Biomed Mater*. 2015;51:260–268.

25. Burris TE, Holmes-Higgin DK, Silvestrini TA, Scholl JA, Proudfoot RA, Baker PC. Corneal asphericity in eye bank eyes implanted with the intrastromal corneal ring. *J Refract Surg*. 1997;13(6):556–567.

26. Torquetti L, Arce C, Merayo-Lloves J, et al. Evaluation of anterior and posterior surfaces of the cornea using a dual Scheimpflug analyzer in keratoconus patients implanted with intrastromal corneal ring segments. *Int J Ophthalmol*. 2016;9(9):1283–1288.

27. Pérez-Escudero A, Dorronsoro C, Marcos S. Correlation between radius and asphericity in surfaces fitted by conics. *J Opt Soc Am A*. 2010;27(7):1541.

28. Utine CA, Ayhan Z, Engin CD. Effect of intracorneal ring segment implantation on corneal asphericity. *Int J Ophthalmol*. 2018;11(8):1303–1307.

29. Piñero DP, Alió JL, El Kady B, Pascual I. Corneal aberrometric and refractive performance of 2 intrastromal corneal ring segment models in early and moderate ectatic disease. *J Cataract Refract Surg*. 2010;36(1):102–109.

30. Siganos D, Ferrara P, Chatzinikolas K, Bessis N, Papastergiou G. Ferrara intrastromal corneal rings for the correction of keratoconus. *J Cataract Refract Surg*. 2002;28(11):1947–1951.

31. Miranda D, Sartori M, Francesconi C, Allemann N, Ferrara P, Campos M. Ferrara intrastromal corneal ring segments for severe keratoconus. *J Refract Surg*. 2003;19(6):645–653.

32. Mohebbi M, Hashemi H, Asgari S, Bigdeli S, Zamani KA. Visual outcomes after femtosecond-assisted intracorneal MyoRing implantation: 18

months of follow-up. *Graefe's Arch Clin Exp Ophthalmol*. 2016;254(5):917–922.

33. Torquetti L, Berbel R, Ferrara P. Long-term follow-up of intrastromal corneal ring segments in keratoconus. *J Cataract Refract Surg*. 2009;35(10):1768–1773.

34. Cheng X, Bradley A, Thibos LN. Predicting subjective judgment of best focus with objective image quality metrics. *J Vis*. 2004;4(4):310–321.

35. Sabesan R, Yoon G. Neural compensation for long-term asymmetric optical blur to improve visual performance in keratoconic eyes. *Investig Ophthalmol Vis Sci*. 2010;51(7):3835–3839.

36. Sabesan R, Barbot A, Yoon G. Enhanced neural function in highly aberrated eyes following perceptual learning with adaptive optics. *Vision Res*. 2017;132:78–84.

37. Sawides L, Dorronsoro C, Haun AM, Peli E, Marcos S. Using Pattern Classification to Measure Adaptation to the Orientation of High Order Aberrations. *PLoS One*. 2013;8(8): e70856.

38. Sawides L, de Gracia P, Dorronsoro C, Webster MA, Marcos S. Vision is adapted to the natural level of blur present in the retinal image. *PLoS One*. 2011;6(11):e27031.

39. Vinas M, Sawides L, de Gracia P, Marcos S. Perceptual adaptation to the correction of natural astigmatism. *PLoS One*. 2012;7(9):e46361.

40. Vinas M, De Gracia P, Dorronsoro C, et al. Astigmatism impact on visual performance: Meridional and adaptational effects. *Optom Vis Sci*. 2013;90(12):1430–1442.

41. Carracedo G, Recchioni A, Alejandre-Alba N, et al. Signs and Symptoms of Dry Eye in Keratoconus Patients Before and After Intrastromal Corneal Rings Surgery. *Curr Eye Res*. 2017;42(4):513–519.

42. Sandes J, Stival LRS, de Ávila MP, et al. Clinical outcomes after implantation of a new intrastromal corneal ring with 140-degree of arc in patients with corneal ectasia. *Int J Ophthalmol*. 2018;11(5):802–806.

43. Lisa C, Fernández-Vega Cueto L, Poo-López A, Madrid-Costa D, Alfonso JF. Long-Term Follow-up of Intrastromal Corneal Ring Segments (210-Degree Arc Length) in Central Keratoconus with High Corneal Asphericity. *Cornea*. 2017;36(11):1325–1330.

44. Ferrara P, Torquetti L. Clinical outcomes after implantation of a new intrastromal corneal ring with a 210-degree arc length. *J Cataract Refract Surg*. 2009;35(9):1604–1608.